星形成ゼミ

SF Newsletter 336
#16 ~ #23
担当:川邊
2021.03.05

SF news letter 336: #16 - #23

16. **Rotating filament in Orion B: Do cores inherit their angular momentum from their parent filament?**
Cheng-Han Hsieh, Héctor G. Arce, Diego Mardones, Shuo Kong, Adele Plunkett Angular momentum is one of the

17. **A search for radio jets from massive young stellar objects. Association of radio jets with H2O and CH3OH masers**
U. Kavak, A. Sanchez-Monge, A. Lopez-Sepulcre, R. Cesaroni, F. F. S. van der Tak, L. Moscadelli, M. T.

18. **Interactions of a shock with a molecular cloud at various stages of its evolution due to thermal instability and gravity**
M. M. Kupilas, C. J. Wareing, J. M. Pittard, S. A. E. G. Falle Using the adaptive mesh refinement code MG, we

19. **Viscous Heating and Boundary Layer Accretion in the Disk of Outbursting Star FU Orionis**
Aaron Labdon, Stefan Kraus, Claire L Davies, Alexander Kreplin, John D Monnier, Jean-Baptiste Le Bouquin,

20. **Chemically tracing the water snowline in protoplanetary disks with HCO^+**
M. Leemker, M. L. R. van 't Hoff, L. Trapman, M. L. van Gelder, M. R. Hogerheijde, D. Rufz-Rodríguez,

21. **Inferring (Sub)millimeter Dust Opacities and Temperature Structure in Edge-on Protostellar Disks From Resolved Multi-Wavelength Continuum Observations: The Case of the HH 212 Disk**
Zhe-Yu Daniel Lin, Chin-Fei Lee, Zhi-Yun Li, John Tobin, Neal Turner (Sub)millimeter dust opacities are required

22. **ALMA View of the Infalling Envelope around a Massive Protostar in S255IR SMA1**
Sheng-Yuan Liu, Yu-Nung Su, Igor Zinchenko, Kuo-Song Wang, Dominique M. -A. Meyer, Yuan Wang, I-Ta

23. **Discovery of a mid-infrared protostellar outburst of exceptional amplitude**
P. W. Lucas, J. Elias, S. Points, Z. Guo, L. C. Smith, B. Stecklum, E. Vorobyov, C. Morris, J. Borissova,

20

Chemically tracing the water snowline in protoplanetary disks with HCO^+

M. Leemker[1], M. L. R. van 't Hoff[1,2], L. Trapman[1], M. L. van Gelder[1], M. R. Hogerheijde[1,3], D. Ruíz-Rodríguez[4], and E. F. van Dishoeck[1,5]

[背景]
- 惑星の形成は雪線(特にH_2Oの雪線)の近くでenhanceされる
- H_2O自身の観測は地上からは困難(大気H_2Oの影響)であるので、代替方法が必要
- 一方、HCO^+の気相での組成は、H_2Oのfreeze-outにより増加。H_2Oの雪線の代わりに用いることが可能(先行研究)。

[研究目的・手法]
- H_2Oの雪線のトレーサーとしてHCO^+や光学的に薄い$H^{13}CO^+$の有用性を調べる。Herbig Ae disk の温度構造を熱化学コード"DALI"でモデル化
- $H^{13}CO^+$とHCO^+ J=2-1輝線についてプロファイルをモデル化(ALMA archival dataと比較可)

[結果と結論]
- HCO^+ や$H^{13}CO^+$組成は、雪線の外側(r=4.5 au)で2auの幅で2桁ジャンプする
- $H^{13}CO^+$とHCO^+では、リング状の構造になる。以下の3つの効果が効く:
  1) 気相のH_2Oにより壊される、2) dust opacity効果、3) 励起効果
- (0.05"分解能ALMA J=2-1 profileとの比較を想定)、中心部では、$H^{13}CO^+$とHCO^+: 組成は、13%, 24%しか低下しない。
- バースト天体V883 Ori case: 雪線がr>40auにあれば、雪線のトレーサーとしてHCO^+は、上記の"制限" は無いと予想。ALMA band 6 HCO^+ => 雪線が100 au 付近にあれば観測と整合する
- (結論)中心部では、HCO^+組成減少は、上記2)、3)の効果のため、1)の効果が顕著では無い。よって、Herbig Ae diskで、HCO^+を用いてH_2Oの雪線を特定することは困難である。バースト天体では、雪線が外側に移動するのでHCO^+利用可

Table 1: DALI model parameters for the disk around a typical Herbig Ae star.

Model parameter	Value
Physical structure	
$R_{\rm subl}$	0.05 AU
$R_{\rm c}$	50 AU
$\Sigma_{\rm c}$	5.8 g cm^{-2}
$M_{\rm disk}$	0.01 $M_\odot$
γ	1
$h_{\rm c}$	0.1
ψ	0.25
Dust properties	
χ	0.2
$f_{\rm ls}$	0.85
$\Delta_{\rm gas/dust}$	100
Stellar spectrum[(1)]	
Type	Herbig
$L_\star$	36 $L_\odot$
$L_{\rm X}$	8(28) erg s^{-1}
$T_{\rm eff}$	1(4) K
$T_{\rm X}$	7(7) K
$\zeta_{\rm c.r.}$	5(-17) s^{-1}
Stellar properties	
$M_\star$	2.3 $M_\odot$
Observational geometry	
i	38°
d	100 pc

Notes. $a(b)$ represents $a \times 10^b$. [(1)] Spectrum of HD 100546 (Kama et al. 2016), which is well approximated by a 10^4 K black body spectrum.

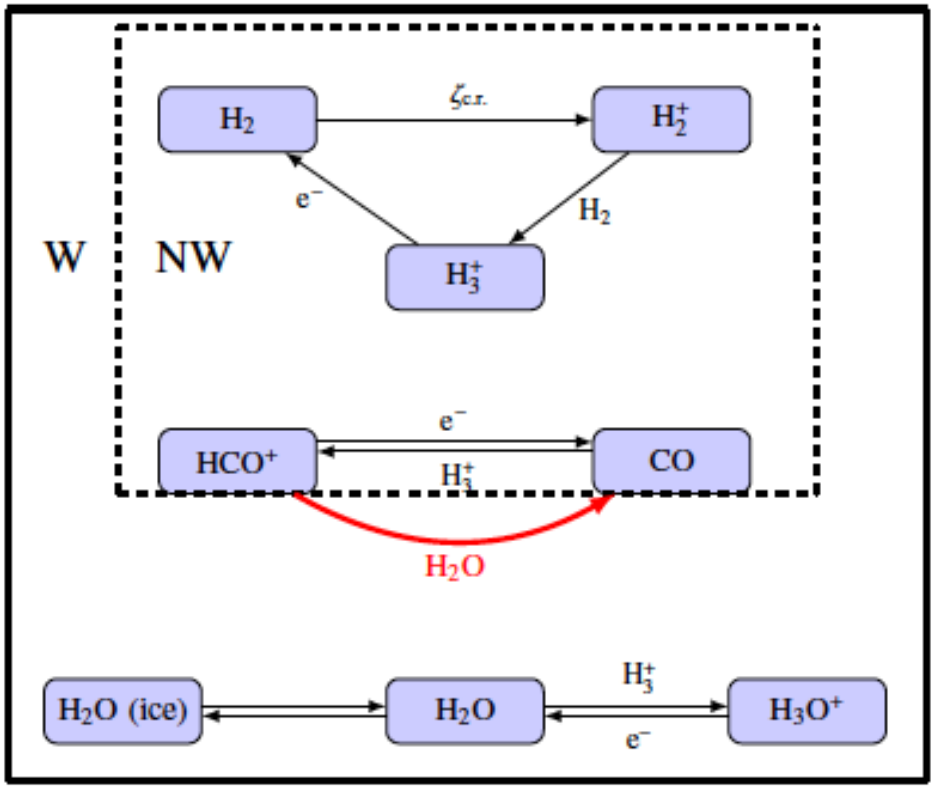

Fig. 2: A schematic view of chemical networks NW (no water) and W (water) used to predict the abundance of HCO^+. The first network, network NW, only includes the reactions enclosed in the dashed box. The second network, network W, includes all reactions present in the figure. The destruction of HCO^+ by gas-phase water is indicated with the thick red arrow.

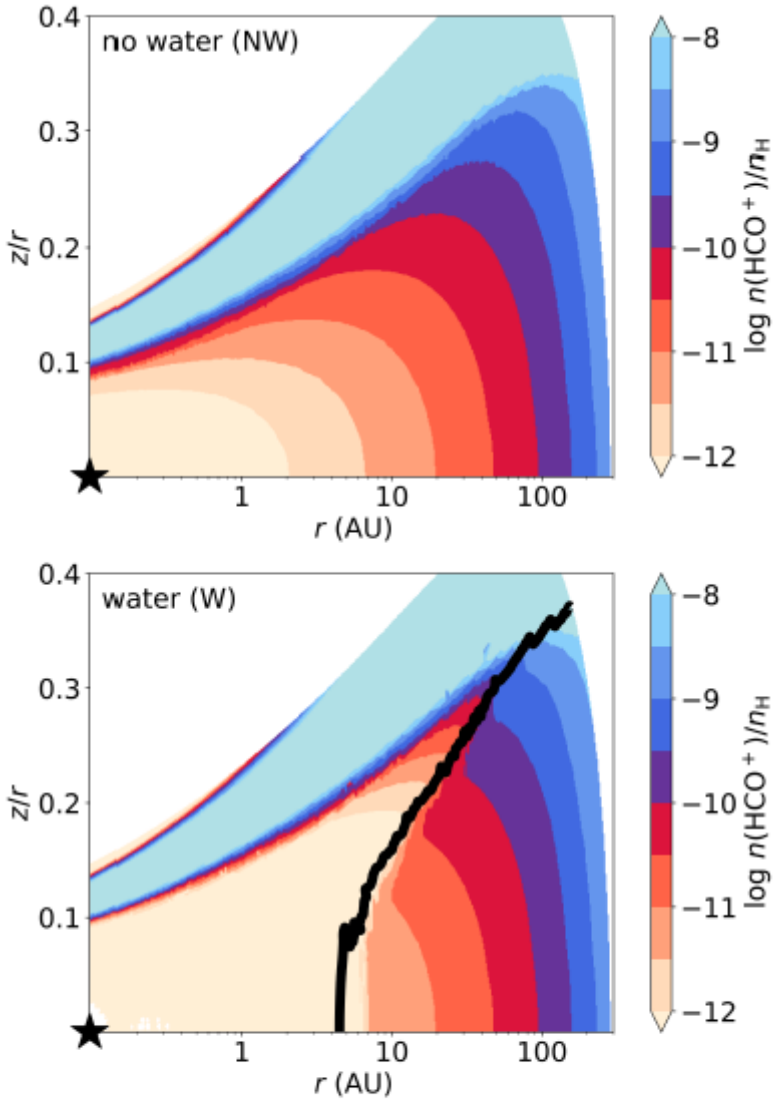

Fig. 3: HCO^+ abundance calculated using chemical network NW (top) and network W (bottom). The water snow surface is marked with the black line in the bottom panel. The position of the star in indicated with the symbol of a black star.

モデル計算の結果
(Herbig Ae)

Low opacity model
=> Kv' =Kv x 10^{-10}

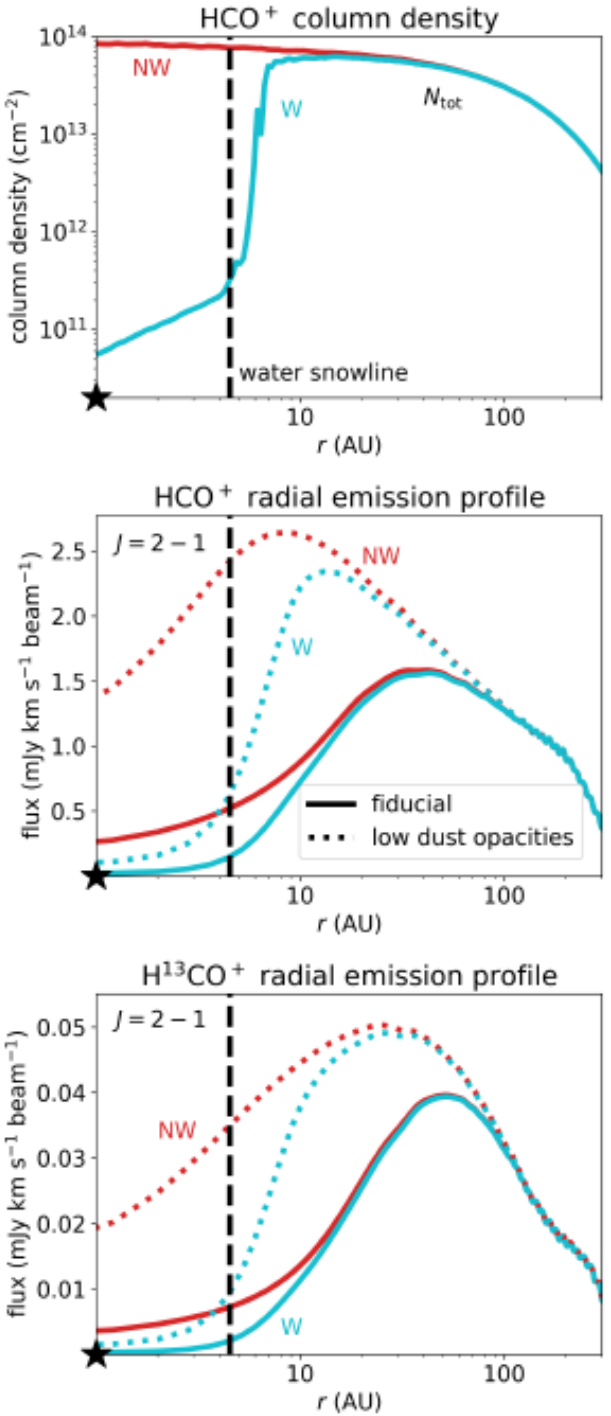

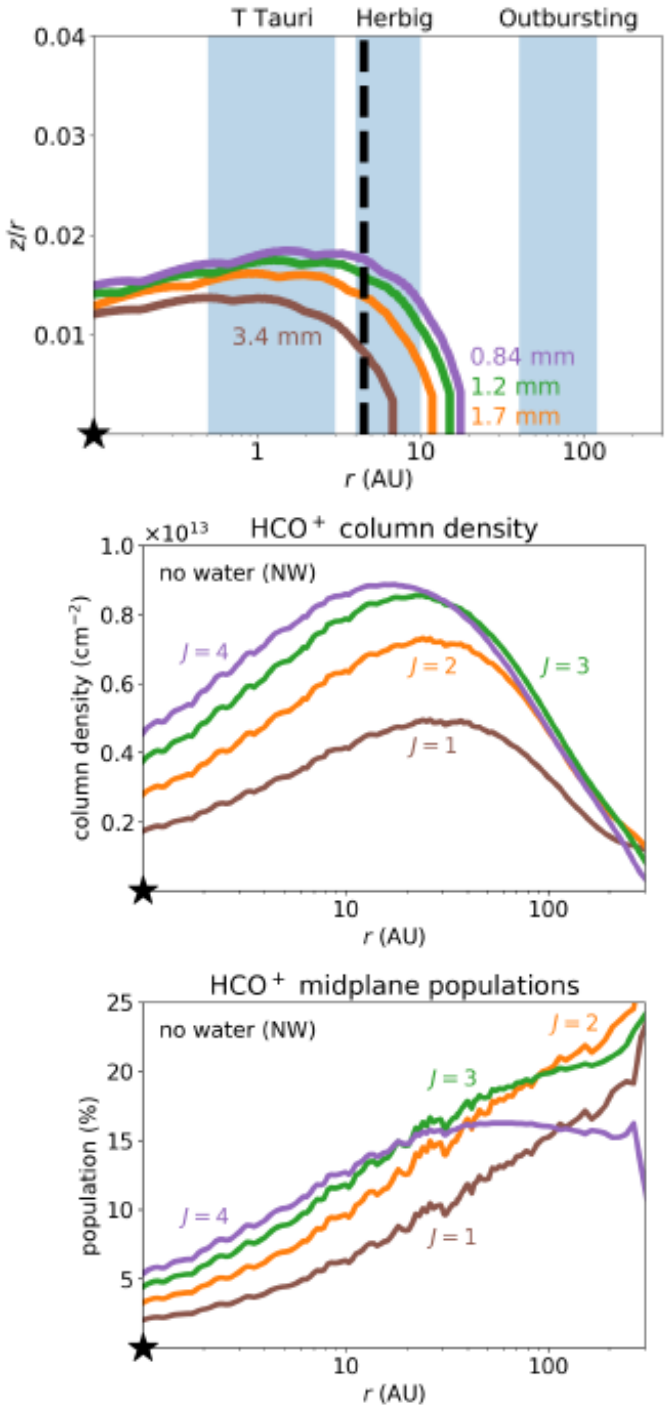

Herbig Ae モデル計算

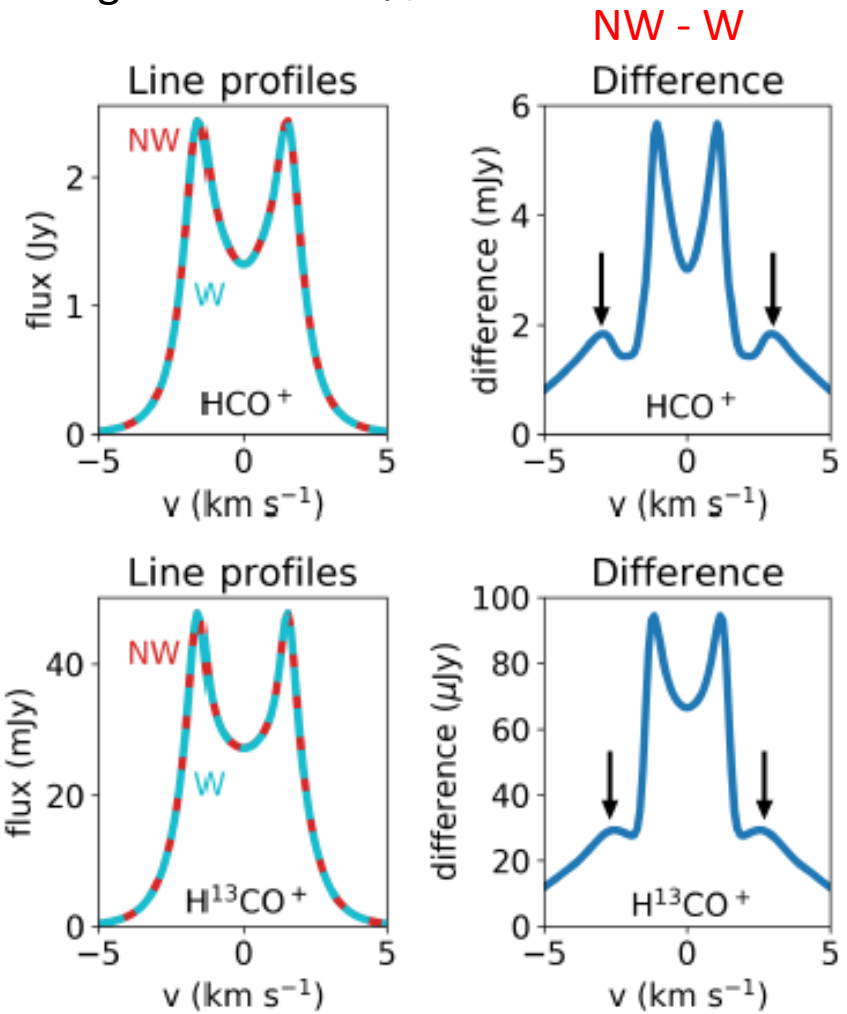

Fig. 8: Left panels: line profile for the $J = 2 - 1$ transition of HCO^+ (top) and $H^{13}CO^+$ (bottom) for chemical network NW (red) and W (light blue). Right panels: difference between the line profiles in the left column. The black arrows indicate where the effect of the water snowline is expected. Note the differences in the vertical axes.

差は小さく、検出困難

V883 Ori のALMA観測

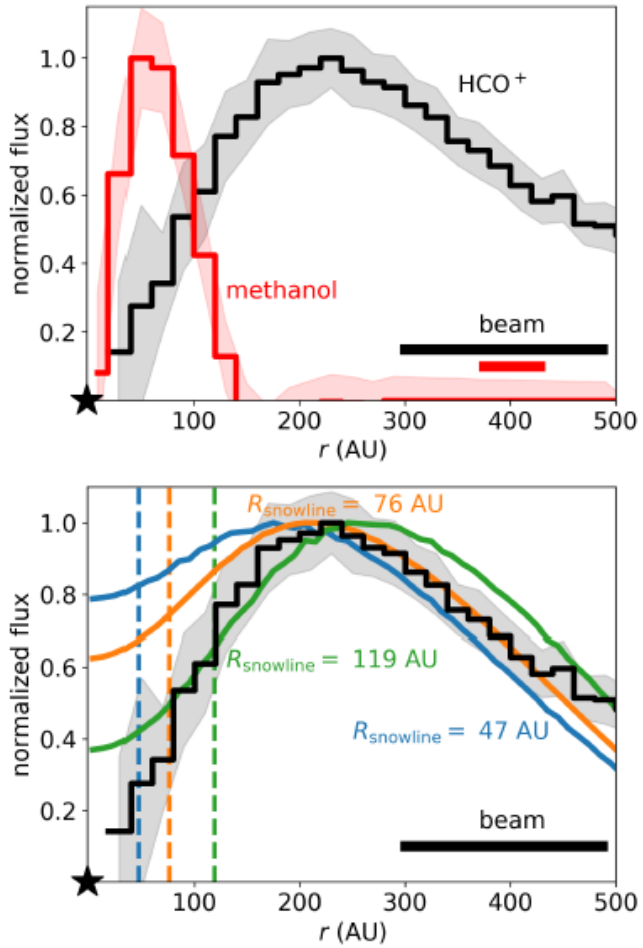

Fig. 10: Top: normalized azimuthal average of the observed HCO^+ $J = 3 - 2$ flux in V883 Ori (black; Ruíz-Rodríguez et al. in prep. and this work) and methanol 18_3-17_4 flux (red; van 't Hoff et al. 2018b). Bottom: normalized azimuthal average of the observed HCO^+ flux (black; as in top panel) and modelled HCO^+ flux for a snowline at 47 AU (blue), 76 AU (orange) and 119 AU (green). The snowline locations of the models are indicated with dashed lines in corresponding colors. The position of the star is indicated with a black star and the beam is indicated by the black bar in the bottom right corner.

モデル計算 (V883 Ori: NW & W): HCO+ J=3-2
(下段白線は、H2O snow line位置)

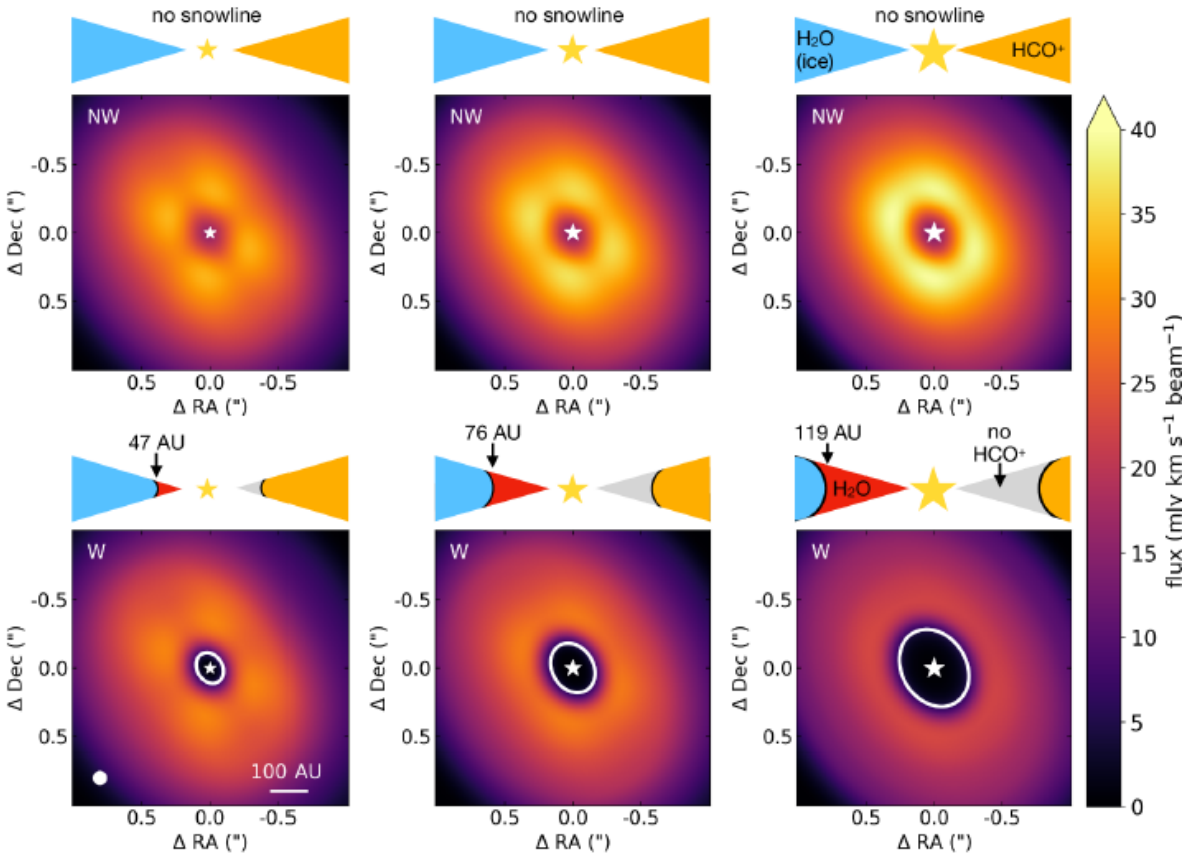

THE ASTROPHYSICAL JOURNAL, 904:181 (17pp), 2020 December 1

22

ALMA View of the Infalling Envelope around a Massive Protostar in S255IR SMA1

Sheng-Yuan Liu[1], Yu-Nung Su[1], Igor Zinchenko[2], Kuo-Song Wang[1], Dominique M.-A. Meyer[3], Yuan Wang[4], and I-Ta Hsieh[1]

[1] Institute of Astronomy and Astrophysics, Academia Sinica, 11F of ASMAB, AS/NTU No.1, Sec. 4, Roosevelt Road, Taipei 10617, Taiwan

[背景]

- 大質量YSOであるS255IRS NIRS3 (SMA1 コア中: d = 1.78 kpc) の光度バーストが、最近観測された。中心星質量~ 20 M_{sun}
- その光度バーストは、円盤が介在した降着変化に起因すると考えられている。中心星の周りのガスの性質を調べることは不可欠

[研究目的・手法]

- バースト起源を探る上で中心星周囲ガスの性質を調べることは不可欠
- ALMAで900μm連続波、CH_3CN J=19-18 K=0-10 輝線を高分解能観測。0.14” 分解能 (=> 250 auに対応)

[結果と結論]

- CH_3CNは、1800 auの広がり(NW-SE方向)を持ち、ほぼ分子流に垂直。
- 中心星周りで、高密度(a few x 10^9 cm^{-3})で熱い(~ 400 K)ガスを確認
- 質量降着率 ~ a few x 10^{-4} M_{sun} yr^{-1}
- 星への降着やJet/outflow駆動に関わるケプラー円盤(があるとすれば)は125 au より小さく、ALMA観測では分解不可だった。

CH_3CN J=19-18 K=3 (コントアー)
PA = 165方向に伸びた構造
900 μm 連続波(カラースケール)
CO outflow direction: 矢印

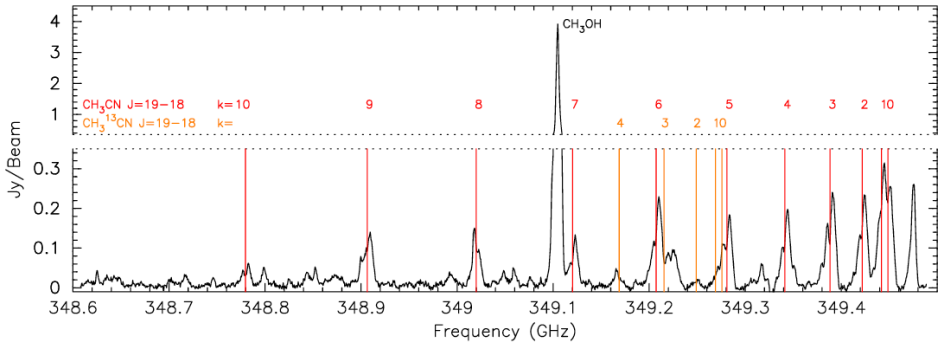

Figure 2. Full spectrum toward the S255IR SMA1 continuum peak at 0″.14 resolution. The CH_3CN $J = 19-18$, $K = 0$ to $K = 10$ lines and the $CH_3^{13}CN$ $J = 19-18$, $K = 0$ to $K = 4$ lines are marked by the red and orange vertical lines, respectively.

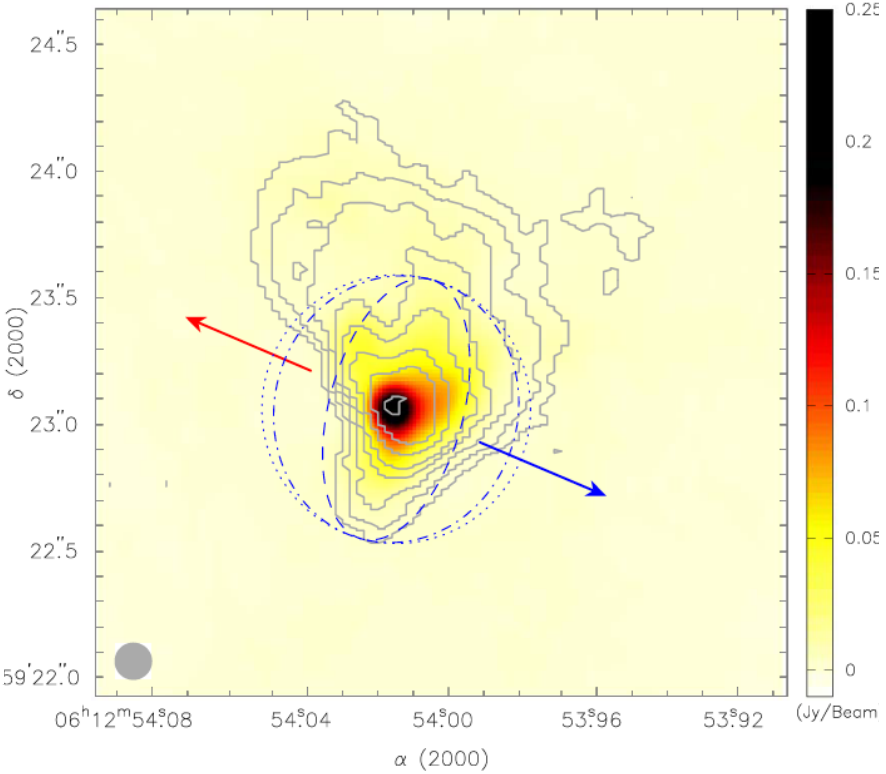

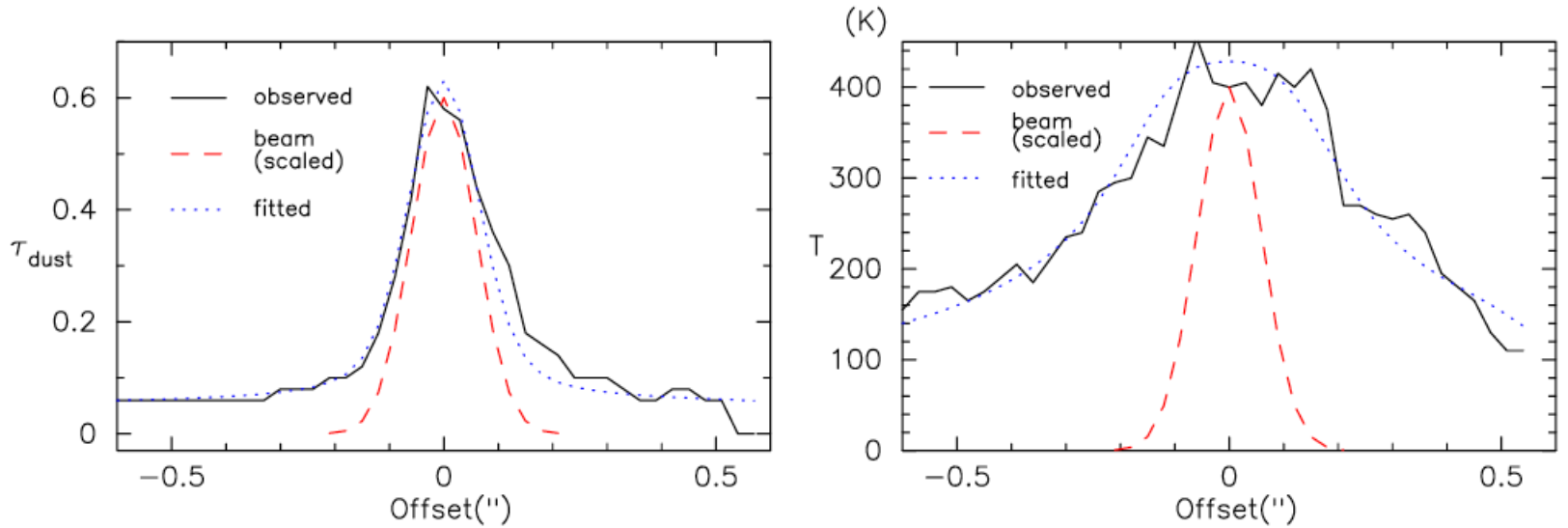

Figure 6. Profiles of physical parameters, including the dust optical depth (which is proportional to the gas column density; left panel) and the gas temperature of the S255IR SMA1 region (right panel).

Spectral Fitによる物理量分布

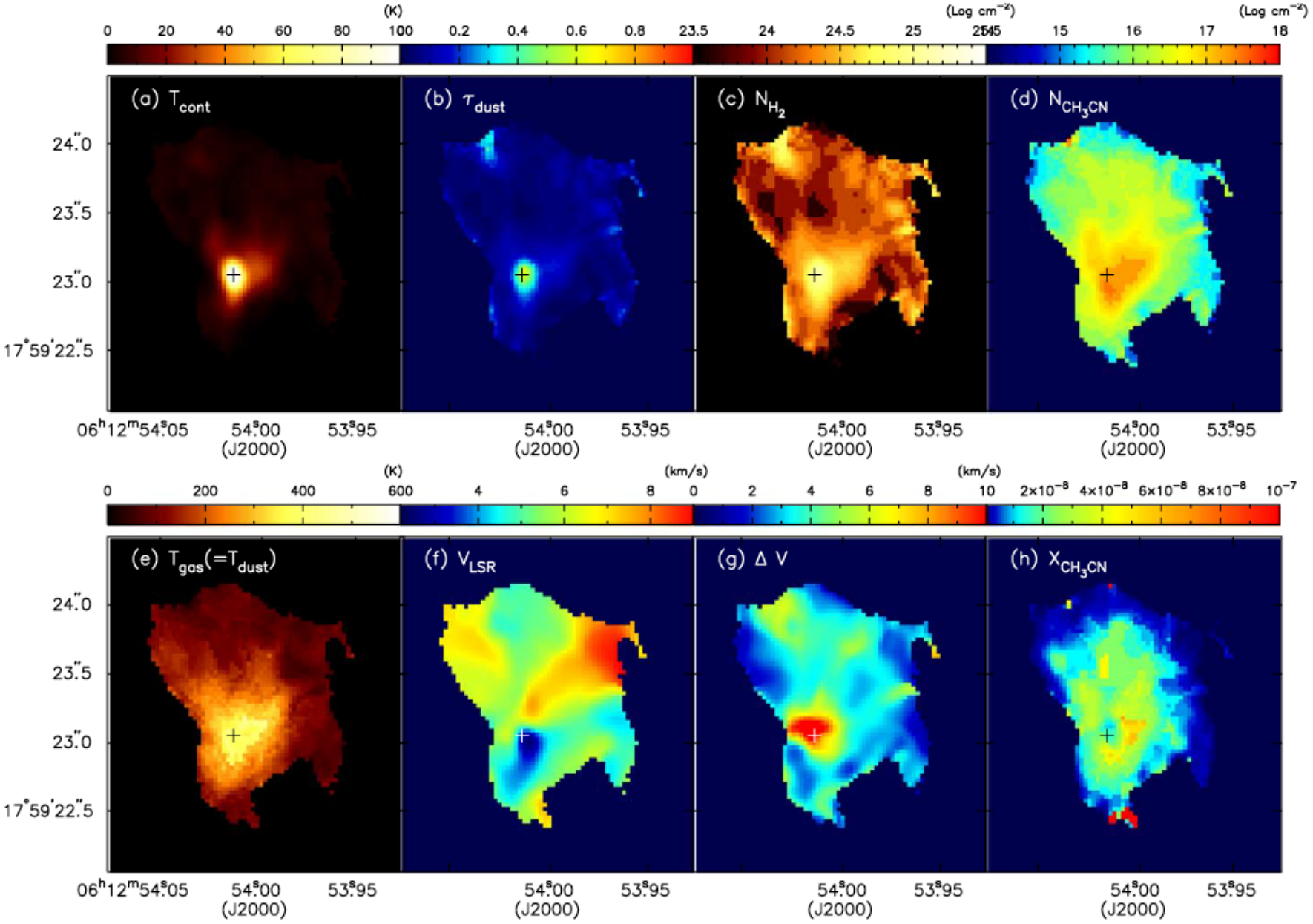

Disk vs Envelope?

Luminoisty ~ 2.4 x 10^4 Lsun
Central massive YSO => ~ 20 M_{sun}

Table 2
Radiative Transfer Model Parameters

Model Parameters	Model 1 (M1)	Model 2 (M2)	Model 3 (M3)	Model 4 (M4)
Central stellar mass	20 $M_\odot$	4.8 $M_\odot$	4.8 $M_\odot$	4.8 $M_\odot$
Inclination angle	25°	60°	60°	60°
Surface density profile		$r^{-1.1}$		
Surface density (at 900 au)	2.0×10^{23} cm^{-2} (0.79 g cm^{-2})	1.8×10^{23} cm^{-2} (0.71 g cm^{-2})	1.8×10^{23} cm^{-2} (0.71 g cm^{-2})	1.8×10^{23} cm^{-2} (0.71 g cm^{-2})
Temperature profile		$\begin{cases} 430\ \mathrm{K} & : \quad r < 214\ \mathrm{au} \\ 430\,(r/214)^{-0.7}\ \mathrm{K} & : \quad r \geqslant 214\ \mathrm{au} \end{cases}$		
Velocity profile	Keplerian	Keplerian	Keplerian + infall	Ulrich
X[CH_3CN]		2×10^{-8}		
Turbulent velocity		2 km s^{-1}		

Infall: ballistic trajectory仮定

Model 4が良さそう

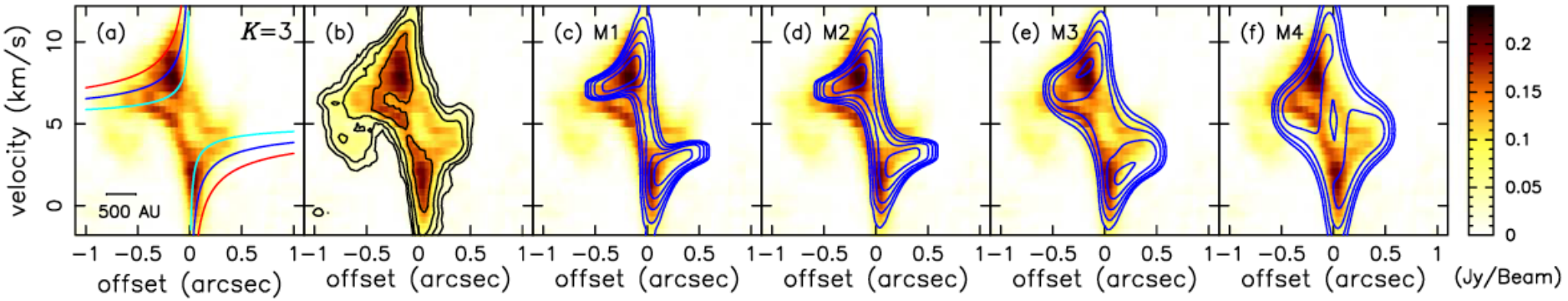

Figure 9. P–V diagram of S255IR SMA1 in the CH_3CN $J = 19-18$ $K = 3$ transition along the P.A. of 165° in false color in all panels. The red, blue, and green curves in panel (a) depict, respectively, the velocity profiles of Keplerian rotation of $(8.04/\sin^2 i)\ M_\odot$, $(3.57/\sin^2 i)\ M_\odot$, and $(0.89/\sin^2 i)\ M_\odot$, where i is the inclination angle of the system. The black contours in panel (b) represent the observed emission at levels of 3, 6, 12, and 24 × 6 mJy beam^{-1} ($=2\sigma$). The blue contours in panels (c)–(f) represent the modeled emission for Model 1, 2, 3, and 4, respectively, also at the same levels as in panel (b). See Section 3.5 for more details.

Model 4と、種々のK-ladderでのPVとの比較
Higer-KでもModel 4でよく説明される：中心のKepler円盤の兆候なし

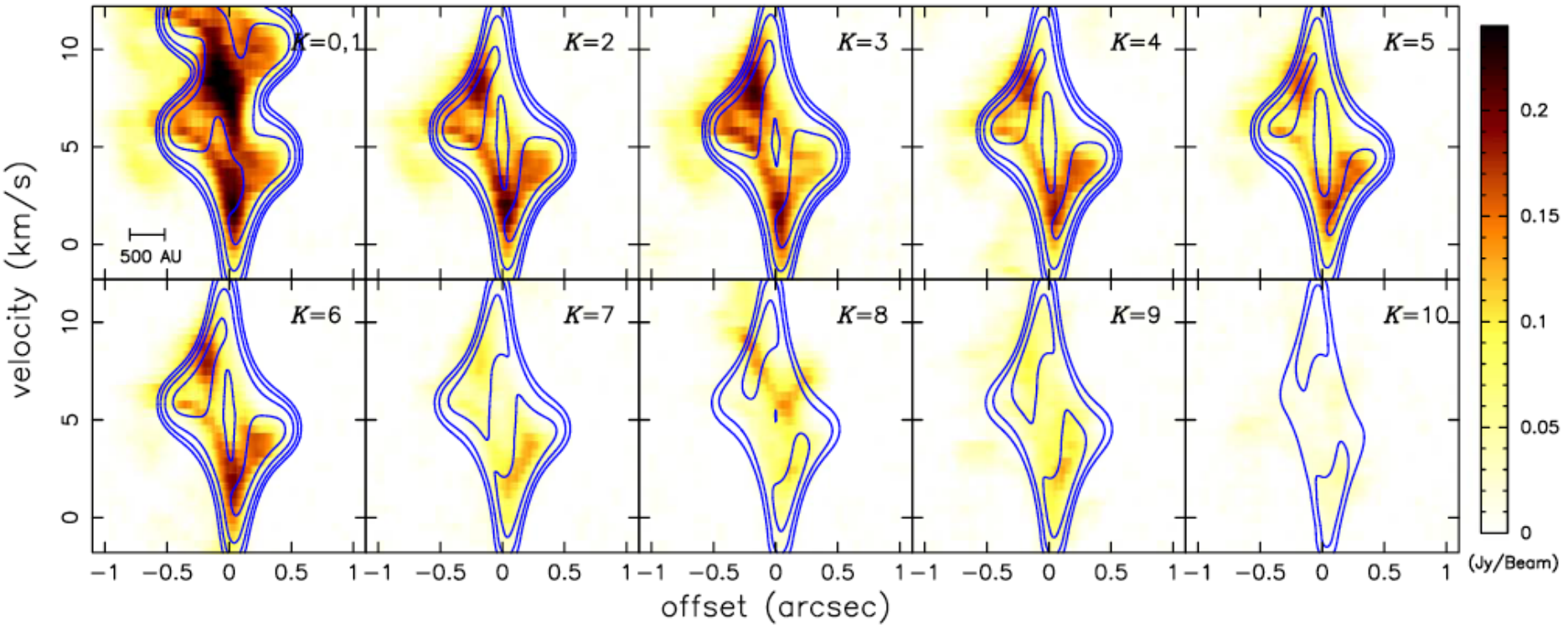

Figure 10. Similar to Figure 8, the *P–V* diagram of S255IR SMA1 in the CH_3CN $J = 19–18$ *K*-ladder along the P.A. of 165°. The observed intensities are shown in false color, and the modeled intensities from Model 4 (M4) are shown with contours. The contour levels are at 3, 6, 12, and 24 × 6 mJy beam^{-1} (=2σ), the same as Figure 8. The *K* component is labeled in the upper right corner of each panel, and the length of a physical scale of 500 au is labeled in the top left panel.

16. **Rotating filament in Orion B: Do cores inherit their angular momentum from their parent filament?**

Cheng-Han Hsieh, Héctor G. Arce, Diego Mardones, Shuo Kong, Adele Plunkett Angular momentum is one of the

N2D+ ALMA 観測

Specific Angular Momentum
半径依存性

$(4 \times 10^{20}\ \mathrm{cm^2\,s^{-1}})$

$(j(r) \propto r^{1.83})$

回転エネルギー/重力エネルギー

$(\beta_{rot} \sim 0.04)$

フィラメントの角運動量は、周囲のガスのTurbulence起源と考えて良い

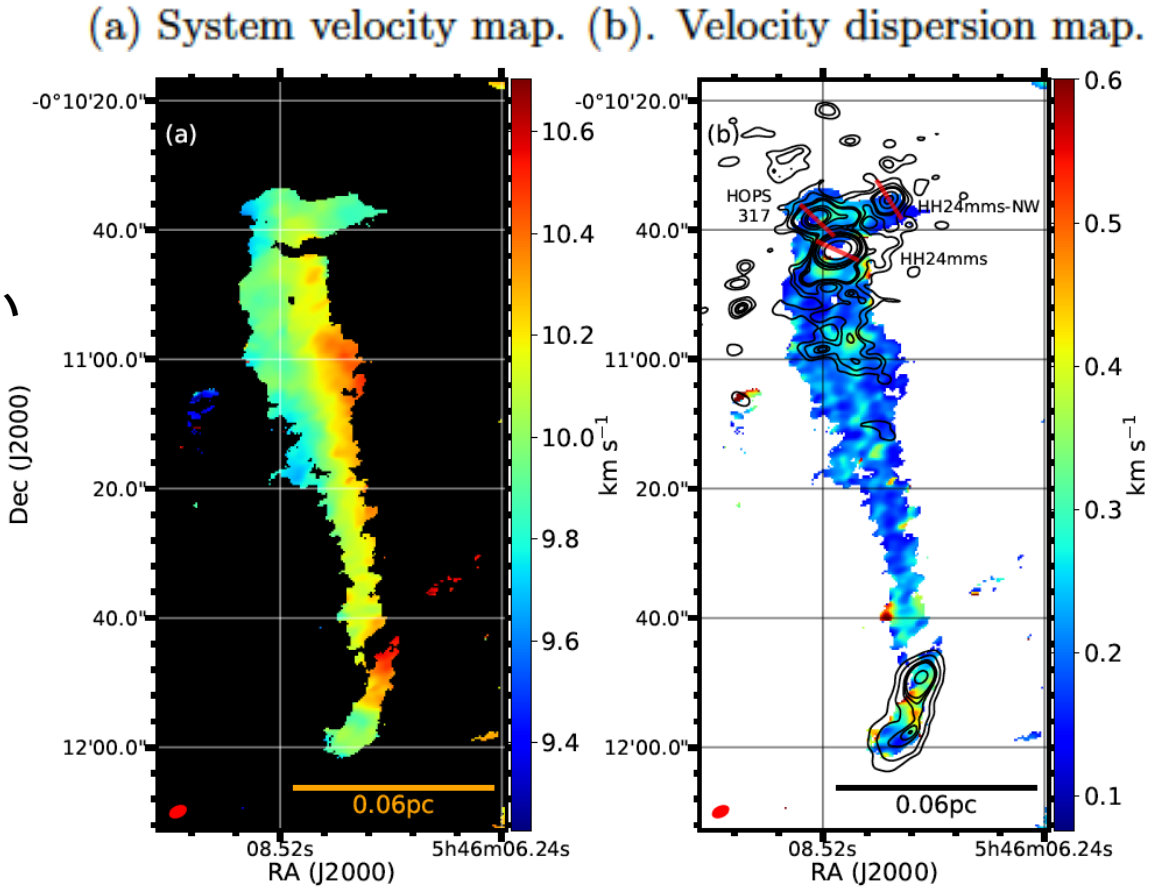

17. **A search for radio jets from massive young stellar objects. Association of radio jets with H2O and CH3OH masers**

U. Kavak, A. Sanchez-Monge, A. Lopez-Sepulcre, R. Cesaroni, F. F. S. van der Tak, L. Moscadelli, M. T.

[背景]
大質量星形成の観測と理論：低質量星形成の相似性?
最近の理論モデルでは、140 M_{sun}まで、disk-mediated accretion in disk jet systems
このシナリオでは、radio jetが大質量星形成領域で共通に見られるはず
[観測・結果]
JVLAで18の大質量星形成領域の観測を実施(6 cm, 1 秒角分解能)
146のradio continuum sourcesを見出した。
その内、28はradio jet candidatesで、さらに7つは most probable radio jets.
7-36 % のradio jet candidatesは、non-thermal radio emission/H_2Oが付随。
＝＞ non-thermal/H_2O maserは、strong shockに付随するのでは。
CH3OH maserに付随するradio jet candidateは、thermal winds and jetsであろう。
[結論]
radio continuum sourceの60%が、radio jet 候補。残りは、HII 領域
大質量星形成領域では、<u>より進化した天体・領域で、radio jetが検出確率高い</u>

18. **Interactions of a shock with a molecular cloud at various stages of its evolution due to thermal instability and gravity**

M. M. Kupilas, C. J. Wareing, J. M. Pittard, S. A. E. G. Falle Using the adaptive mesh refinement code MG, we

ABSTRACT

This is a pre-copyedited, author-produced PDF of an article accepted for publication in *Monthly Notices of the Royal Astronomy Society* following peer review.

Using the adaptive mesh refinement code MG, we perform hydrodynamic simulations of the interaction of a shock with a molecular cloud evolving due to thermal instability and gravity. To explore the relative importance of these processes, three case studies are presented. The first follows the formation of a molecular cloud out of an initially quiescent atomic medium due to the effects of thermal instability and gravity. The second case introduces a shock whilst the cloud is still in the warm atomic phase, and the third scenario introduces a shock once the molecular cloud has formed. The shocks accelerate the global collapse of the clouds with both experiencing local gravitational collapse prior to this. When the cloud is still atomic, the evolution is shock dominated and structures form due to dynamical instabilities within a radiatively cooled shell. While the transmitted shock can potentially trigger the thermal instability, this is prevented as material is shocked multiple times on the order of a cloud crushing time-scale. When the cloud is molecular, the post-shock flow is directed via the pre-existing structure through low-density regions in the inter-clump medium. The clumps are accelerated and deformed as the flow induces clump-clump collisions and mergers that collapse under gravity. For a limited period, both shocked cases show a mixture of Kolmogorov and Burgers turbulence-like velocity and logarithmic density power spectra, and strongly varying density spectra. The clouds presented in this work provide realistic conditions that will be used in future feedback studies.

Key words: Hydrodynamics – Instabilities – ISM: clouds – shock waves – turbulence – methods: numerical

19. **Viscous Heating and Boundary Layer Accretion in the Disk of Outbursting Star FU Orionis**

Aaron Labdon, Stefan Kraus, Claire L Davies, Alexander Kreplin, John D Monnier, Jean-Baptiste Le Bouquin,

赤外線干渉計(?)で FU-Oriのau-scale diskを分解して観測 (J & H bands 同時)

=> inner disk temp. $T \propto r^{-0.74\pm0.02}$.

Viscos heatingで予想されるdisk温度構造と $T \propto r^{-0.75}$ と一致

ABSTRACT

Context. FU Orionis is the archetypal FUor star, a subclass of young stellar object (YSO) that undergo rapid brightening events, often gaining 4-6 magnitudes on timescales of days. This brightening is often associated with a massive increase in accretion; one of the most ubiquitous processes in astrophysics from planets and stars to super-massive black holes. We present multi-band interferometric observations of the FU Ori circumstellar environment, including the first J-band interferometric observations of a Y SO.

Aims. We investigate the morphology and temperature gradient of the inner-most regions of the accretion disk around FU Orionis. We aim to characterise the heating mechanisms of the disk and comment on potential outburst triggering processes.

Methods. Recent upgrades to the MIRC-X instrument at the CHARA array allowed the first dual-band J and H observations of YSOs. Using baselines up to 331 m, we present high angular resolution data of a YSO covering the near-infrared bands J, H, and K. The unprecedented spectral range of the data allows us to apply temperature gradient models to the innermost regions of FU Ori.

Results. We spatially resolve the innermost astronomical unit of the disk and determine the exponent of the temperature gradient of the inner disk to $T \propto r^{-0.74\pm0.02}$. This agrees with theoretical work that predicts $T \propto r^{-0.75}$ for actively accreting, steady state disks, a value only obtainable through viscous heating within the disk. We find a disk which extends down to the stellar surface at 0.015 ± 0.007 au where the temperature is found to be 5800 ± 700 K indicating boundary layer accretion. We find a disk inclined at $32 \pm 4°$ with a minor-axis position angle of $34 \pm 11°$.

Conclusions. We demonstrate that J-band interferometric observations of YSOs are feasible with the MIRC-X instrument at CHARA. The temperature gradient power-law derived for the inner disk is consistent with theoretical predictions for steady-state, optically thick, viciously heated accretion disks.

Key words. Stars: individual: FU Orionis – Techniques: interferometric – Accretion disks

21

Inferring (sub)millimetre dust opacities and temperature structure in edge-on protostellar discs from resolved multiwavelength continuum observations: the case of the HH 212 disc

Zhe-Yu Daniel Lin [1,2,3★] Chin-Fei Lee,[2,4] Zhi-Yun Li,[1] John J. Tobin[5] and Neal J. Turner[6]
[1]*Department of Astronomy, University of Virginia, Charlottesville, VA 22904, USA*

[背景]

- (サブ)ミリ波塵オパシティ(Kv)は、塵放射強度から(塵)質量の導出に不可欠だが、これまで、その値は若い星の周りの円盤等ではよくわかっていなかった。

[研究目的・手法]

- エッジオン円盤において、Kv= τo,v / ($\rho_0 R_0$)として、Kvに制限する方法を提案。

  $\tau_{o,v}$: 光学的厚み。円盤の面に沿って測った強度から導出

  ρ_0 : 円盤の重力的な安定性から導出

  R_0 : 円盤の半径(outer edge)
- 1 D モデル+ 2D (RADMAC-3Dベース)を Class 0天体 HH212 円盤 (ALMA bands 9,7,3 & VLA 波長9.1 mm) に適用した。

[結果と結論]

- Kv~ 1.9 x 10^{-2} (band 7), 1.3 x10^{-2} (band6; 1.3mm), 4.9 x 10^{-3} (band3) $cm^2 g^{-1}$
- 結果は、よく用いられる”処方”式　Kv = 2.3 x 10^{-2} (1.3mm/λ) をサポート。

23. **Discovery of a mid-infrared protostellar outburst of exceptional amplitude**

P. W. Lucas, J. Elias, S. Points, Z. Guo, L. C. Smith, B. Stecklum, E. Vorobyov, C. Morris, J. Borissova,

WISE Class-I YSO (d=2.6 kpc) within IRDC

Peak Accretion Rate ~ 10^{-4} $M_{sun}yr^{-1}$, => L_{bol} = a few x 10^2 L_{sun}

(consistent with classical FU-Ori event?)

4.6 μm peak => T= 800-1000 K at a disk location R ~ 4.5 au

No hotter matter expected from 熱不安定性 or MRI

=> edge-on diskで隠されている? Or disc fragmentation?

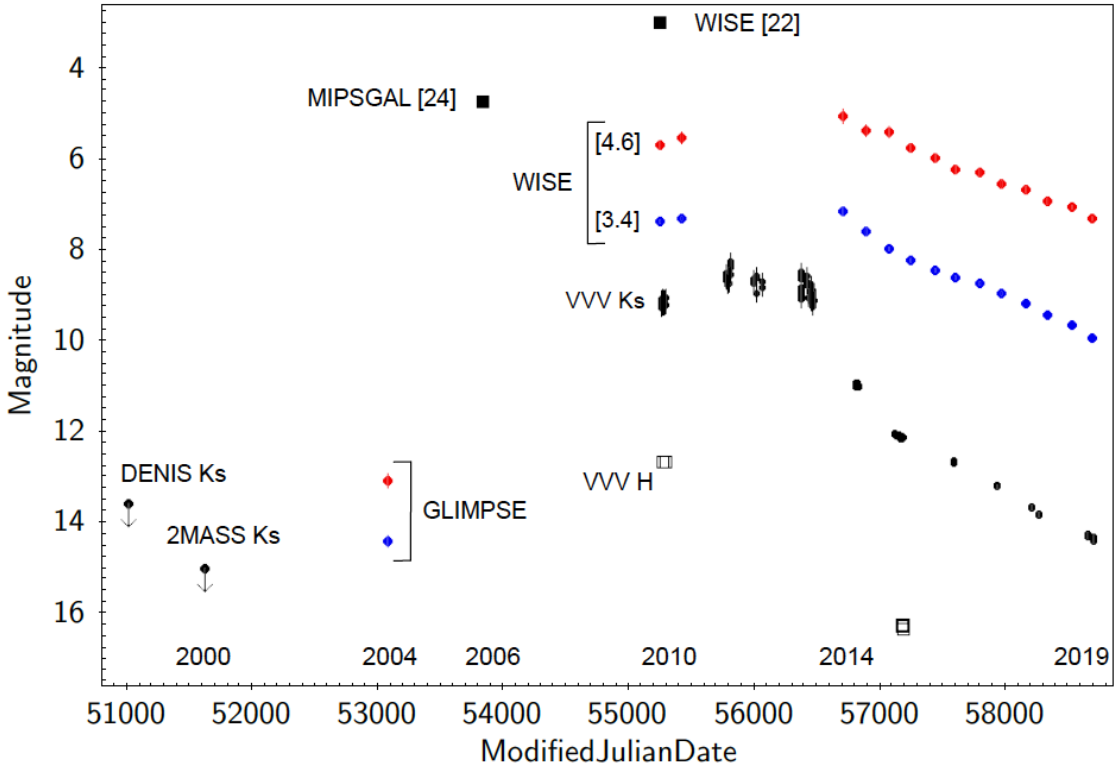

SED